Ultrasonics - Sonochemistry 61 (2020) 104824

Contents lists available at ScienceDirect

Ultrasonics - Sonochemistry

journal homepage: www.elsevier.com/locate/ultson

High-performance sono/nano-catalytic system: Fe_3O_4@Pd/$CaCO_3$-DTT core/shell nanostructures, a suitable alternative for traditional reducing agents for antibodies

Reza Taheri-Ledari[a], Ali Maleki[a,*], Ehsan Zolfaghari[a], Maral Radmanesh[a], Hodjattallah Rabbani[b], Ali Salimi[b], Ramin Fazel[c]

[a] Catalysts and Organic Synthesis Research Laboratory, Department of Chemistry, Iran University of Science and Technology, Tehran 16846-13114, Iran
[b] Monoclonal Antibody Research Center, Avicenna Research Institute, ACECR, Tehran, Iran
[c] Livogen Pharmed, Research and Innovation Center, Tehran, Iran

ARTICLE INFO

Keywords:
Antibody reduction
Dithiothreitol
Herceptin
Magnetic nanoparticles
Sonochemistry
Synergistic catalytic effect

ABSTRACT

Herein, a novel heterogeneous nanoscale reducing agent for antibody cleavage, made of iron oxide nanoparticles, silica network, palladium on calcium carbonate (10%), and dithiothreitol (Fe_3O_4@Pd/$CaCO_3$-DTT), is presented as a substantial alternative for traditional homogeneous analogues. Conventionally, antibody fragmentation is accomplished using reducing agents and proteases that digest or cleave certain portions of the immunoglobulin protein structure to provide active thiol sites for drug tagging aims. Then, dialysis process is needed to separate excess chemical structures and purify the reduced antibody. In this work, we have made an effort to design a suitable heterogeneous tool for protein cleavage and skip the dialysis process for purification of the reduced antibody. In this regard, firstly, various preparation methods including microwave irradiation, reflux and ultrasonication have been precisely compared, and it has been proven that the best result is obtained through 10 min ultrasound (US) irradiation using an US bath with 50 KHz frequency and 200 $W L^{-1}$ power density. Then, all the necessary structural analyses have been done and thoroughly interpreted for the final product. Afterward, the catalytic performance of Fe_3O_4@Pd/$CaCO_3$-DTT nanoscale system in the presence of US waves (50 KHz, 200 W) has been monitored using some disulphide derivatives. The NPs could be conveniently separated from the mixture through their substantial paramagnetic property. Thus, dialysis process in which various types of membranes are used is practically jumped after the reduction process. In this work, this is clearly demonstrated that there is a constructive synergistic effect between US waves and prepared Fe_3O_4@Pd/$CaCO_3$-DTT nanoscale reducing agent. Ultimately, trastuzumab (anti HER-2) antibody has been used to test the performance of the prepared Fe_3O_4@Pd/$CaCO_3$-DTT NPs in a real protein reduction reaction.

1. Introduction

Recently, attentions to conjugated drugs, which are constructed of a biosynthetic protein chain and a chemical structure, has been increased due to their higher efficacy and lower negative side effects than the chemical agents [1,2]. This category of high-tech pharmaceuticals are widely studied nowadays. According to the final structure of this generation of therapeutic agents, amide, disulfide, ester or thioester connections are employed at the main site of conjugation [3]. One of the well-known species of the protein-conjugated drugs, is antibody-drug conjugates (ADCs) that are mostly used for cancer-targeted therapy [4]. To prepare an ADC, amine group (coming from side chain of lysine) and thiol group (coming from cysteine), provide appropriate chemical active sites for biochemical conjugation [1–4]. Site-specification is also considered as another strategy which could provide various new sites for conjugation reactions [5]. Since, there are several disulfide bonds in the antibody's framework, several thiol sites could be resulted from reducing the antibodies, as the proper active sites for the conjugation. For this purpose, a partial reduction of S–S bonds by a mild reductant such as dithiothreitol (DTT) (Cleland's reagent), tris-(2-carboxyethyl) phosphine (TCEP) and 2-mercaptoethanol is needed [6,7]. Then, some purification processes like dialysis is needed to separate the reductant from discrete antibodies [8].

Functionalized iron oxide nanoparticles (Fe_3O_4 NPs) are extremely

---

Abbreviations: US, ultrasound; MW, microwave; NPs, nanoparticles; DTT, dithiothreitol; TRA, trastuzumab

[*] Corresponding author.

E-mail address: maleki@iust.ac.ir (A. Maleki).

https://doi.org/10.1016/j.ultsonch.2019.104824
Received 24 August 2019; Received in revised form 2 October 2019; Accepted 3 October 2019
Available online 08 October 2019

used as considerable heterogeneous nanoscale catalysts in chemical and biochemical reactions, due to their magnetic core and shells with functionalization capability [9,10]. One of the most efficient methods for surface functionalization of NPs is ultrasonication that provides a proper driving force for chemical reactions and gives us more satisfying results about physical properties of desired product [11–13]. This field of study also investigates the effect of ultrasound (US) waves on uniformity of the new layers loaded onto the surface of NPs [14]. In addition, both morphology and particle size of the modified NPs are well controlled via ultrasonication in comparison with other methods. Thus, in this work, ultrasonication was used as an eco-friendly and convenient procedure for the fabrication of the uniform NPs. The first and foremost reason for using the US irradiation, instead of other methods such as microwave (MW) and stirring under reflux condition is that the other approaches do not give us the acceptable results. For instance, Maktedar, et al. compared US irradiation with stirring method to prepare graphene oxide, and found out that more desirable result is obtained using US wave irradiation. In addition, they achieved desired products in shorter times without using additive hazardous compounds [15]. As another sample, Liu, et al. have compared ultrasonication with stirring in production of polyaniline by using various analyses such as X-ray diffraction, energy dispersive X-ray and transmission electron microscopy [16]. The obtained results implied that the crystallinity of polyaniline produced via ultrasonication was considerably higher than that produced via the stirring. Ultrasonication is cheaper, faster and more effective method for preparation of heterogeneous NPs in liquid phase in comparison with other methods. From physical aspect, ultrasonication creates an effective vibration that can form a monodispersed heterogeneous mixture and inhibit aggregation of the particles. From chemical aspect, high-energy bubbles created by US waves (cavitation) into a water bath provide the required energy for reactants to occur a chemical reaction [17]. This phenomenon occurs when the fast vibration of the probe produces numerous bubbles in micro-scale.

In this study, firstly, we present a novel strategy for preparation of DTT-functionalized silica coated Fe_3O_4 NPs (Fe_3O_4@Pd/$CaCO_3$-DTT) via ultrasonication, then its application is precisely investigated for S–S bond reduction. A precise comparison between the different methods has been made for preparation of the nanocomposite and this is demonstrated that ultrasonication is the most efficient method for this purpose. In this regard, an ultrasonic bath with frequency 50 KHz and power density 200 W L^{-1} has been suitably applied. Then, to show high catalytic performance of Fe_3O4@Pd/$CaCO_3$-DTT nanocomposite, initially a model reaction of S–S reduction by the prepared heterogeneous nano-reductant was executed using diphenyl disulfide, and the optimal conditions was indicated. Afterward, the catalytic performance Fe_3O_4@Pd/$CaCO_3$-DTT has been more investigated using different disulfide derivatives such as bis(4-chlorophenyl) disulfide and bis(4-methylphenyl) disulfide. Finally, the catalytic activity of the novel designed reducing agent is monitored in a real antibody reduction on trastuzumab (Herceptin) antibody which is an IgG1 monoclonal antibody. The characterization of the desired nanoscale product such as general structure, size and morphology, surface functionalization ratio, magnetic property, biological features and crystal pattern were comprehensively investigated, as well. This novel nano-organocatalyst could be a substantial alternative for homogeneous S–S bond reducing agents through its significant properties. By using this product, dialysis process is eliminated after reduction of antibodies and they would be easily purified by using an external magnet. Here, to prepare the Fe_3O_4@Pd/$CaCO_3$-DTT NPs, a convenient strategy is presented in which palladium deposited on calcium carbonate (Pd/$CaCO_3$), known as Lindlar catalyst, and US waves are employed. Also, through the precise comparisons, this has been disclosed that there is a great synergistic catalytic effect between the fabricated Fe_3O_4@Pd/$CaCO_3$-DTT NPs and US waves.

2. Results and discussion

2.1. Preparation

To initiate our study, Fe_3O_4 NPs were synthesized according to the literature [18]. Firstly, iron salts were dissolved in distilled water at 80 °C. Then, ammonia solution was added dropwise until $pH = 12$ was achieved. Dark particles of Fe_3O_4 were collected by an external magnet in the bottom of the flask and were washed for several times with distilled water and ethanol. From here onwards, to obtain more uniform particles and also to inhibit the agglomeration of the particles, the preparation process was continued by US waves. In the next stage, Fe_3O_4 NPs were coated by silicate network by using of tetraethyl orthosilicate (TEOS). A TEOS solution (20 wt%) were dropwise added to the finely dispersed mixture of Fe_3O_4 NPs in polyethylene glycol (PEG-300), distilled water and ethanol, during sonication [19–21]. Light brown silica-coated iron oxide NPs (Fe_3O_4@SiO_2) were magnetically collected, washed and dried at 40 °C.

Lindlar catalyst is a heterogeneous catalyst that is formed from palladium deposited on calcium carbonate then poisoned with various forms of lead or sulphur, and used for hydrogenation of alkynes to alkenes [22]. As an advanced form of this reagent, palladium NPs were prepared and immobilized on calcium carbonate, then was used for coupling reaction through the presence of palladium NPs. This type of Pd particles help us to have monodispersed Pd particles on a substrate and use them for various aims without need to design difficult strategies. The electronic interactions with oxygen atom is considered as one the most important properties of Pd, as well [23,24]. In this work, Pd NPs were simultaneously prepared and immobilized on calcium carbonate via US wave irradiation, because we needed an appropriate resource to provide driving force for both production and immobilization with acceptable uniformity onto the surface of Fe_3O_4@SiO_2 NPs. In this regard, different methods such as reflux condition, high temperature and pressure into an autoclave and MW irradiation were also experimented, and the obtained results were compared with US-assisted method (Table 1). The obtained results exhibited that the core/shell structure of Fe_3O_4@SiO_2 NPs was damaged at high temperatures, and MW was not an appropriate method due to its low performance. Therefore, as the next stage of preparation process, we have used Pd/$CaCO_3$ to execute a convenient and high performance core-coating method that was implemented by US waves. In this regard, Fe_3O_4@SiO_2 core/shell NPs were well dispersed in dry tetrahydrofuran (THF) by ultrasonication, then Pd/$CaCO_3$ were added and the mixture was put into an US bath. Time, temperature and frequency are three main factors in NPs coating reactions that were carefully monitored to obtain the optimum conditions by investigating Fourier-transform infrared

Table 1
Comparison of the different methods for preparation of Fe_3O_4@SiO_2@Pd/$CaCO_3$ NPs.

Entry	Method	Temp. (°C)	Conditions	Time (h)	W (%) of S[a]
1	Reflux	64	THF	12	3.8
2	Autoclave	150	DMF	12	1.2
3	MW irradiation	–	THF / P: 300[b]	1	0.8
4	Ultrasonication	0–5	THF / F: 50 KHz, PD: 200 W	2	4.5*

* Optimum condition by considering particle size, uniformity, monodispersity, morphology and surface functionalization ratio (W% of sulfur element).

[a] Weight percentage obtained from EDX and CHNS analyses (Tables S1 and S2 in the SI section).

[b] A conventional microwave oven at a power (P) of 300 W was used; Temp.: temperature; MW-P: MW irradiation power; F: ultrasonication frequency (KHz), PD: ultrasonication power density (W/L), US bath was used for all of the ultrasonication steps; All the reactions were carried out under N_2 atmosphere.

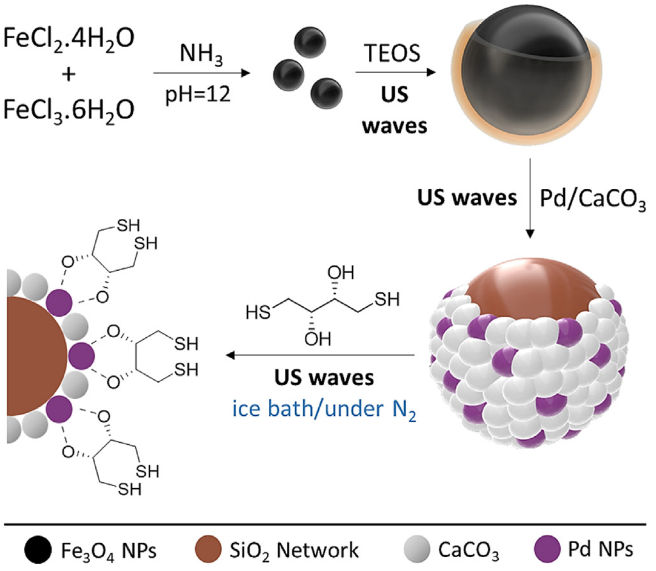

Scheme 1. Preparation route of Fe_3O_4@Pd/$CaCO_3$-DTT NPs, US frequency: 50 KHz and power density 200 W was applied in an ultrasonic bath.

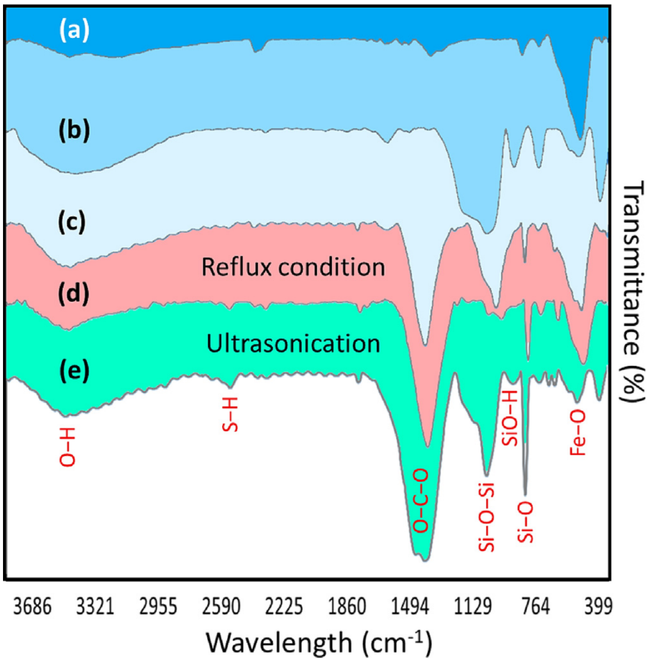

Fig. 1. FT-IR spectra of (a) Fe_3O_4 NPs, (b) Fe_3O_4@SiO_2 core/shell NPs, (c) Fe_3O_4@SiO_2@Pd/$CaCO_3$ NPs synthesized via ultrasonication, (d) Fe_3O_4@SiO_2@Pd/$CaCO_3$ NPs synthesized under reflux condition, and (e) Fe_3O_4@Pd/$CaCO_3$-DTT NPs via ultrasonication.

(FT-IR) and energy dispersive X-ray (EDX) spectroscopic methods. Next, Fe_3O_4@SiO_2@Pd/$CaCO_3$ NPs were magnetically collected and washed for several times with THF. As the last step of the preparation process, Fe_3O_4@SiO_2@Pd/$CaCO_3$ NPs were well dispersed in dry ethanol by using the US bath, then a solution of DTT (0.1 M in dry ethanol) was added dropwise to the mixture over 20 min during ultrasonication (Scheme 1). It should be noted that low temperature and neutral atmosphere are two essential factors at this stage, due to the instability of DTT. The prepared desired product was immediately used in disulfide bond reduction.

2.2. *Characterization*

2.2.1. *FT-IR study*

FT-IR spectra of the produced samples were investigated step by step. As they can be seen in the Fig. 1, the peak related to the stretching vibration of Fe–O bond at ~580 cm^{-1} is observed in the all spectra (a–e). New appeared peaks at ~800, ~940 and ~1100 cm^{-1} coming from the stretching vibrations of Si–O, SiO–H and Si–O–Si bonds, respectively, confirm the formation of the silica network around the magnetic core (spectra b, c and e) [18–20]. Actually, the spectra (c) and (d) show a comparative result obtained via two different methods, ultrasonication and reflux, respectively. From these spectra, it can be easily deduced that the silica network that coated the magnetic core is damaged under reflux conditions. This happening is proven by an intense drop in the peaks related to the silica network at the mentioned areas (spectrum d). However, the absorption peaks of CO_3^{2-} at ~855, ~1082 and ~1455 cm^{-1} are reported to be the common specific peaks of the CO_3^{2-} in $CaCO_3$. In the spectra c–e, a sharp peak at ~855 cm^{-1} is assigned as symmetric stretching, and the peak at ~1082 cm^{-1}, which is in overlapping with the appeared peak at ~1100 cm^{-1}, coming from the silica network and is assigned as out of-plane bending modes of CO_3^{2-}. A broad peak at ~1455 cm^{-1}, assigned as asymmetrical stretching vibration of O–C–O, confirmed the existence of CO_3^{2-} onto the surface of core/shell NPs, as well. Finally, the presence of DTT is confirmed by appeared weak peaks at 2509 cm^{-1} that belongs to thiol groups (spectrum e). The absorption peak related to stretching vibration of C–H bonds with sp3 hybridation in the DTT structure, is covered by broad peak of superficial –OH groups.

2.2.2. *EDX study*

Elemental analysis on the Fe_3O_4@SiO_2@Pd/$CaCO_3$ NPs were done before and after functionalization with DTT. The resulted energy dispersive X-ray (EDX) spectra have been shown in Fig. 2. As it can be seen in spectrum (b), the signal related to sulfur element was appeared at ~2.25 Kev after carrying out the US-assisted surface functionalization with DTT. In addition, the signal intensity of carbon atom was increased after DTT functionalization. Also, the existence of other elements such as oxygen, iron, silicon, calcium and palladium were proven by this method.

2.2.3. *Microscopic imaging study*

Field-emission scanning electron microscopy (FESEM) images of both resulted products from ultrasonication and reflux methods have been illustrated in Fig. 3. As can be seen in image (a), despite the existence of the strong magnetic property, very uniform and monodispersed Fe_3O_4@SiO_2 NPs were obtained via ultrasonication. Obviously, well-separated NPs provide wider active surface areas for catalytic applications. Subsequently, well-coated NPs by Pd/$CaCO_3$ with great spherical morphology were obtained via the same method, as illustrated in image (b). Surface roughness also revealed that Pd/$CaCO_3$ powder have been well distributed onto the Fe_3O_4@SiO_2 NPs surfaces (image c). In contrast, the particle accumulation has been occurred over a longer reaction time under reflux conditions (image d). This intense condition causes a deformation in the spherical shape and also in core/shell structure of Fe_3O_4@SiO_2 NPs. However, agglomeration is always considered as a negative feature for catalytic systems because the catalytic performance would be declined through blocking the active sites. In the other words, more active surface area would be available when NPs are well dispersed and in a uniform size. Moreover, the average particle sizes ca. 42 nm and ca. 47 nm were obtained for the Fe_3O_4@SiO_2 NPs resulted from ultrasonication and reflux methods, respectively (diagrams e). This evaluation on the particle size was performed for 30 particles by Digimizer software. As presented by the size distribution diagrams (Fig. 3e), resulted product from ultrasonication method has more focused in a limited range of 35–45 nm that confirms well uniformity of the fabricated NPs in comparison with the reflux method. The mean size of the fabricated Fe_3O_4@Pd/$CaCO_3$-DTT NPs has also been investigated and ca. 70 nm was determined,

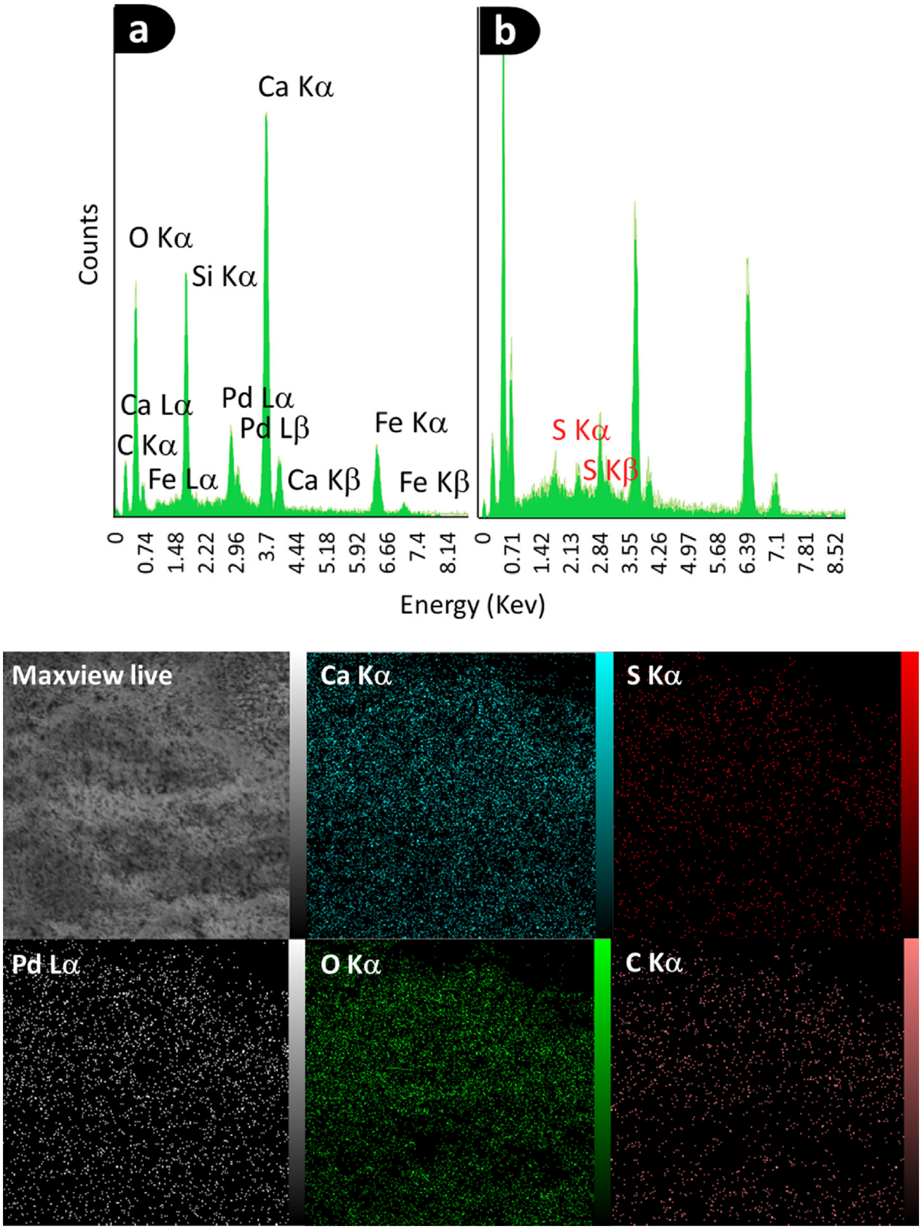

Fig. 2. EDX spectra of (a) Fe_3O_4@Pd/$CaCO_3$ NPs and (b) Fe_3O_4@Pd/$CaCO_3$-DTT NPs NPs, and EDX images of Fe_3O_4@Pd/$CaCO_3$-DTT NPs, synthesized via ultrasonication.

which is more investigated by dynamic light scattering method in the solution phase.

2.2.4. *Dynamic light scattering study*

Intensity-based dynamic light scattering (DLS) measurement prove that despite including a strong magnetic behavior, the finely dispersed Fe_3O_4@Pd/$CaCO_3$-DTT NPs are produced via ultrasonication method. As shown in Fig. 4, a sharp peak with low polydispersity index (PDI) has been appeared in the related spectrum of US-assisted prepared NPs. Additionally, this is confirmed that no particle accumulation is occurred in the solution phase. The mean size of ca. 70 nm is also verified for the fabricated Fe_3O_4@Pd/$CaCO_3$-DTT NPs. This is also exhibited that no desirable result has been obtained from MW irradiation method. This is obtained from a peak appeared at ca. 225 nm that show large sizes of the particles with higher PDI in rather than the US's product. However, this is disclosed that the worst result was obtained via reflux method because two different peaks with high PDIs (1.3) were observed at ca. 150 and 370 nm. These peaks (specially the second one) clearly reveal that abundant accumulations have been occurred for the NPs in the solution phase and even probe-type ultrasonicator (10 min) could not cleave them.

2.2.5. *XRD study*

X-ray diffraction (XRD) pattern of Fe_3O_4@SiO_2@Pd/$CaCO_3$@DTT NPs was prepared and compared with the obtained patterns of Pd/$CaCO_3$ and DTT as the standard materials, as presented in Fig. 5. In accordance with our expectation, no similarity to XRD pattern of Pd/$CaCO_3$ powder (pattern b) was observed for the produced desired product (pattern a). In contrast, the pattern was dramatically similar to DTT pattern (pattern c). It can be easily deduced that the surface of Fe_3O_4@SiO_2@Pd/$CaCO_3$ NPs have been well covered by DTT through the electronic interactions between Pd(II) and oxygen atoms. It means that they are well distributed onto the surface of silica-coated iron oxide NPs through applying US waves and positive interactions between silicon and oxygen atoms present in the silica network and Lindlar agent structures, respectively.

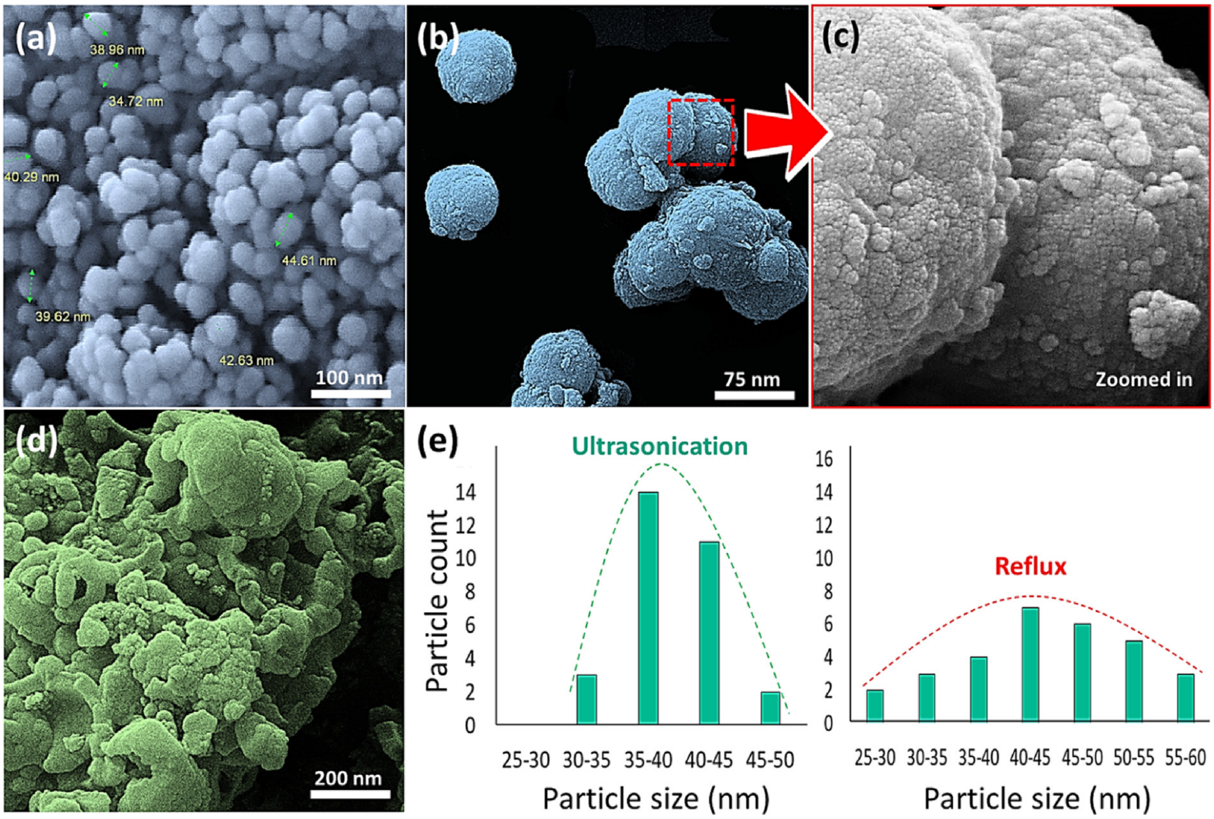

Fig. 3. FESEM images of (a) $Fe_3O_4@SiO_2$ NPs, (b,c) $Fe_3O_4@Pd/CaCO_3$-DTT NPs resulted from ultrasonication method, and (d) and resulted from reflux method, (e) Size distribution diagrams of $Fe_3O_4@SiO_2$ NPs, resulted from ultrasonication and reflux methods, calculated for 30 NPs by Digimizer software.

2.2.6. VSM study

One of the most important advantages of surface-functionalized iron oxide NPs with organic reagents in comparison with their pure organic analogues, is that they are easily separated from the reaction mixture without any need to complex separation processes like dialysis. Through having a magnetic core, they are separable from the mixture after completion of the reaction by using an external magnet. In this regard, in order to investigate magnetic property of $Fe_3O_4@Pd/CaCO_3$-DTT NPs, vibrating sample magnetometer (VSM) analysis was used and the resulted spectra were shown in Fig. 6. As it can be observed, the synthesized iron oxide NPs have shown a typical super-paramagnetic behavior (curve a). It is obvious that the magnetic property is reduced proportional to more core-coating by new layers. Accordingly, the magnetization of $Fe_3O_4@Pd/CaCO_3$-DTT NPs is ca. 33 emu/g decreased after three successive core-coating by TEOS, $Pd/CaCO_3$ and DTT, respectively (curve b).

2.2.7. TGA study

In order to compare the final structure of desired product with silica-coated iron oxide NPs, thermogravimetric analysis (TGA) were done and resulted curves have been shown in Fig. 7. As it can be seen, with increasing the temperature to ca. 95 °C, a partial rise in the weight was observed for both samples. At this temperature, NPs could adsorb moisture onto their hot surfaces. According to the curves, this adsorption was ∼0.7% more for $Fe_3O_4@Pd/CaCO_3$-DTT NPs (curve b) in comparison with $Fe_3O_4@SiO_2$ NPs (curve a), and this is occurred due to the presence of $CaCO_3$ on the surface of desired final product [25]. These adsorbed moisture were separated by increasing the temperature

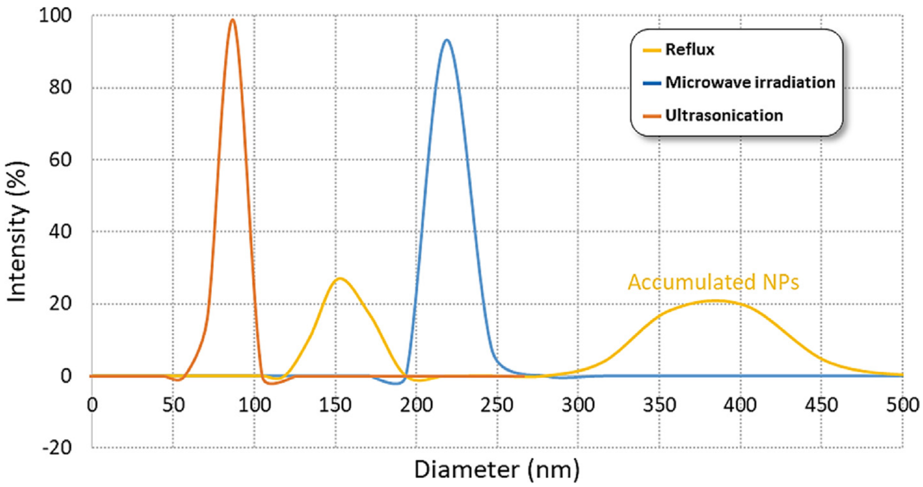

Fig. 4. Dynamic light scattering (DLS) spectra of the fabricated $Fe_3O_4@Pd/CaCO_3$-DTT NPs via ultrasonication, MW irradiation, and reflux methods. The average size of the final product of ultrasonication is ca. 70 nm in diameter while this is ca. 150 nm for reflux's product [ultrasonic probe ultrasonicator was used to disperse samples for 10 min prior to DLS measurements].

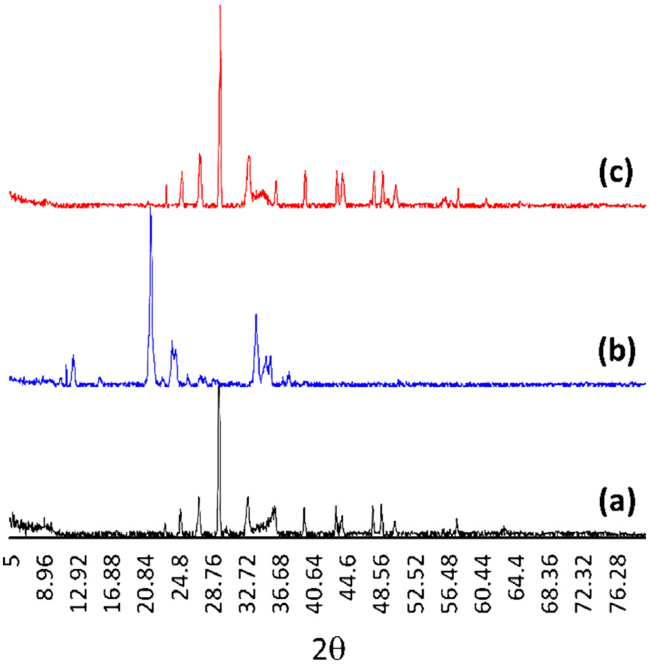

Fig. 5. XRD patterns of Fe_3O_4@Pd/$CaCO_3$-DTT NPs (a), Pd/$CaCO_3$ (b) and DTT (c).

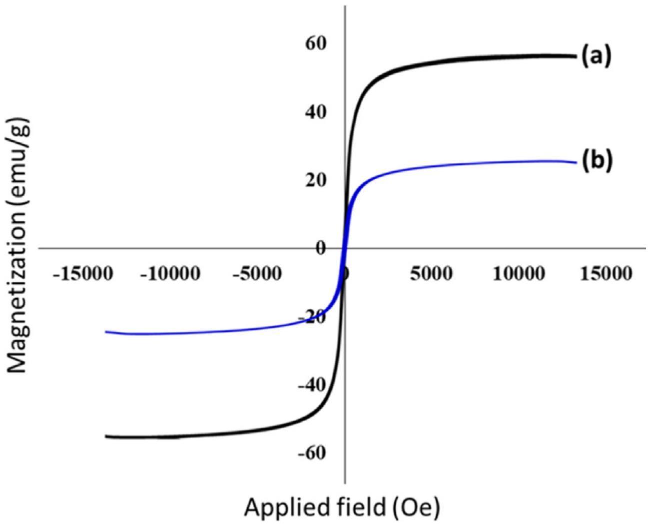

Fig. 6. The room temperature M – H curve of the neat Fe_3O_4 NPs (a) and Fe_3O_4@Pd/$CaCO_3$-DTT NPs (b).

to ca. 110 and ca. 200 °C for Fe_3O_4@Pd/$CaCO_3$-DTT and Fe_3O_4@SiO_2 NPs, respectively, and the main weight loss was initiated at these temperatures. As can be seen in the curve (a), with increasing the temperature to 600 °C, water molecules entrapped into the silica network have left the network and total weight was gradually reduced (ca. 8%). At the temperatures higher than 100 °C, the silica network has likely been damaged, as it had been previously proven by FT-IR spectroscopy. However, since the silica network works as a great molecular sieve, this would be an acceptable weight loss value for Fe_3O_4@SiO_2 NPs at this stage [26,27]. According to the curve (b), with increasing the temperature to 400 °C, ca. 5% weight loss was observed that could be related to losing DTT. At this stage, the partial amounts of water molecules entrapped into the underlying silica network layer are also removed. In continue, proportional to the increasing in the temperature (to above 400 °C), an intense drop was observed in the curve that exhibited ca. 7% weight loss through the elimination of Pd/$CaCO_3$.

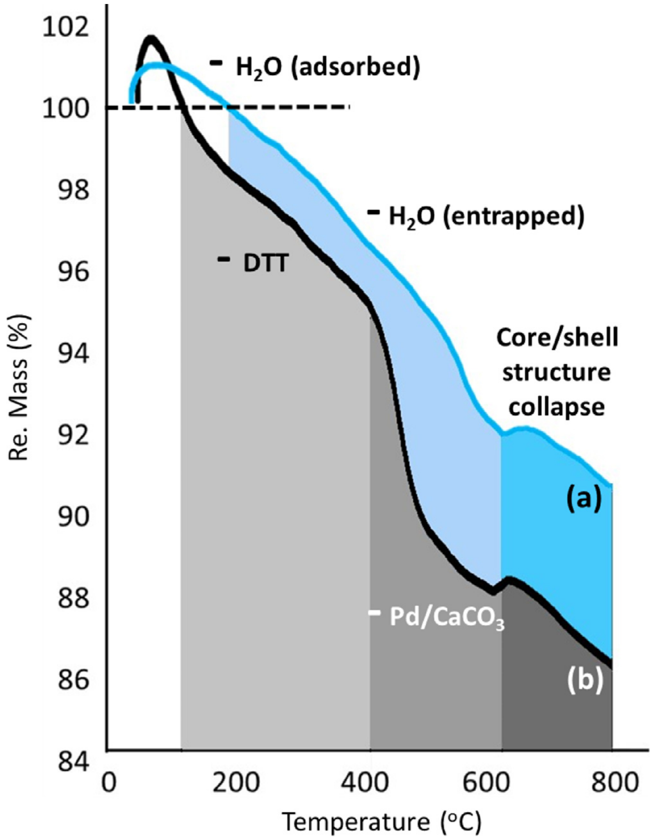

Fig. 7. TGA curves of Fe_3O_4@SiO_2 NPs (a) and Fe_3O_4@Pd/$CaCO_3$-DTT NPs (b).

Ultimately, the main core/shell structure started to collapse in both samples at 600 °C, and quite distinct shoulders were appeared in both curves at this temperature.

2.2.8. Solid state UV–visible spectroscopy study

In order to investigate that DTT is still in dithiol form and disulfide bonding was not occurred during ultrasonication, UV–visible absorption spectra of DTT and Fe_3O_4@Pd/$CaCO_3$-DTT NPs were prepared for products resulted via ultrasonication and stirring under reflux condition. As Fig. 8 implies, the spectrum related to desired product, which was obtained under reflux conditions, exhibited a relatively sharp absorbance peak at 265–325 nm, whereas the product obtained via ultrasonication shows a relatively weak peak at this area. This peak coming from the oxidized DTTs and indicates that despite the reaction was carried out under neutral atmosphere, some of the loaded DTTs onto the surface of NPs were oxidized during 24 h stirring at high temperature [28]. Since, the ultrasonication is executed under faster and milder condition, this oxidation and deactivation of the loaded DTTs has not been significantly occurred.

Among all of the various preparation methods, ultrasonication has provided more suitable conditions for surface-coating and functionalization of the magnetic NPs. In fact, these types of nanoscale materials are inherently prone to form agglomerations due to their super-paramagnetic behavior. Furthermore, their tendency for aggregation is increased when their surfaces are covered by some materials with jelly nature like polymers. As shown in schematic (Fig. 9), regular physical blows, which are created by US waves, lead the particles to be well dispersed in the solution phase that is rich of the coating agent (Pd/$CaCO_3$). In addition, required energy for covalent connections or electronic interactions is provided by the hot bubbles. That is why great surface-functionalization ratio and well uniformity is obtained via this method. In contrast, mechanical stirring leads the magnetic particles to be agglomerated and their surfaces could not be well functionalized.

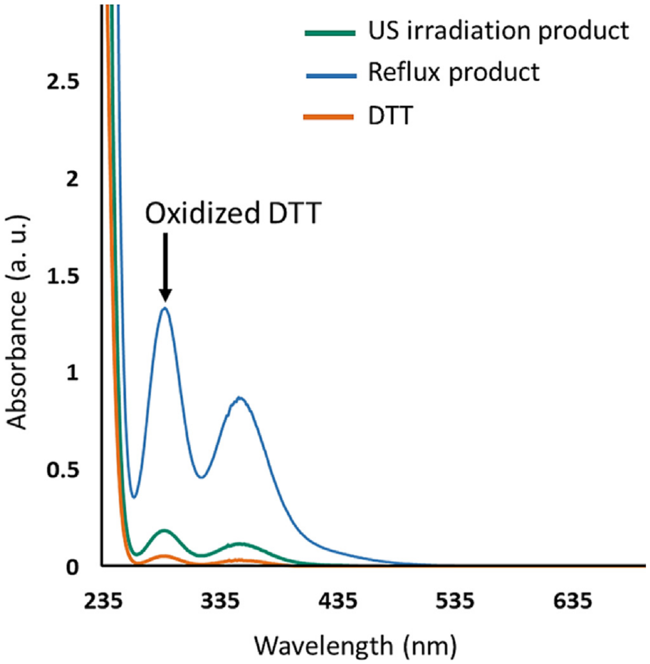

Fig. 8. Solid-state UV–visible absorption spectra of DTT and Fe_3O_4@Pd/$CaCO_3$-DTT NPs, resulted from ultrasonication and reflux condition.

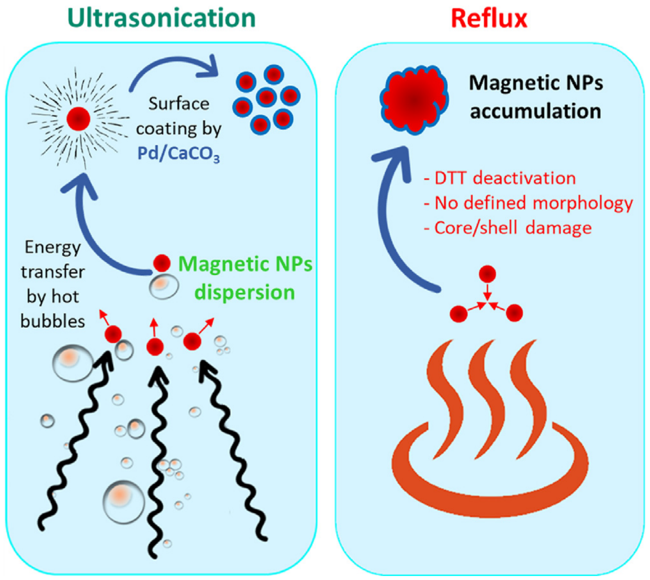

Fig. 9. Schematic comparison between ultrasonication and reflux methods for preparation of Fe_3O_4@Pd/$CaCO_3$-DTT NPs.

Additionally, their core/shell structure and spherical morphology are damaged under intense conditions of the reflux method. Also, the chance of disulfide bond oxidation (deactivation of DTT) is increased because of a longer reaction time at the reflux method.

2.3. Antibody reduction activity

2.3.1. Optimization

In order to obtain the optimum conditions for reducing the antibodies by novel prepared heterogeneous nanoscale reductant, control reactions were carried out using diphenyl disulfide. Since the price of the antibodies is higher than the chemical disulfide derivatives, this model reaction was selected for optimization. For this purpose, Fe_3O_4@Pd/$CaCO_3$-DTT NPs were prepared and freshly used under N_2 atmosphere in dry tetrahydrofuran (THF) at room temperature. Accordingly, the same reaction conditions were applied for all of the control reactions. Different amounts of the magnetic reducing agent, different reaction times, and the synergistic effect between the magnetic NPs and US waves were precisely investigated. As Table 2 reports, the best result was observed when 0.01 g of Fe_3O_4@Pd/$CaCO_3$-DTT was used under 10 min ultrasonication with 50 KHz frequency and 200 W power density. The reaction progress was screened using thin-layer chromatography (TLC), as illustrated in Fig. S1 (in the SI section). After completion of the reduction reaction, the heterogeneous reductant NPs were conveniently collected by using an external magnet, then resulted thiophenol was immediately separated and purified via flash column chromatography and identified with ^1H NMR and ^{13}C NMR (see the SI section). To perform more investigation on the control reactions, bis(4-chlorophenyl) disulfide and bis(4-methylphenyl) disulfide, as two available disulfide derivatives, were also used for reduction reaction at the same optimal conditions. Almost the same reaction yields (~93%) were obtained for these two derivatives after purification process. The resulted 4-chlorobenzenethiol and 4-methylbenzenethiol have been identified through NMR spectroscopy (SI section).

2.3.2. Colorimetric test

The performance of the prepared nanoscale reductant was also studied in a real reduction reaction of trastuzumab (TRA, anti-HER2) that is a humanized IgG1 monoclonal antibody. One of the well-known methods for indicating S-S bond conversion to –SH groups is colorimetric test by Ellman's reagent in which 5,5′-dithio-bis[2-nitrobenzoic acid] (DTNB) is used [29]. In this test, DTNB (as one of the highly active disulfide derivatives) reacts with the free thiol groups that are resulted from the S-S bond cleavage of trastuzumab by Fe_3O_4@Pd/$CaCO_3$-DTT NPs and produce 5-mercapto-2-nitrobenzaldehyde in yellow color. Thus, it could be claimed that the intensity of the yellow color is proportional to the concentration of the provided –SH sites. Accordingly, it can be clearly seen in Fig. 10 that a relatively bold yellow solution was resulted by employing Fe_3O_4@Pd/$CaCO_3$-DTT NPs, after 10 min ultrasonication (image d). It should be noted that the magnetic NPs should be freshly used because the surface DTTs would be oxidized to 1,2-dithiane ring (deactivated form of DTT) during a long-time storage. Image (a) also reveals that no significant change in the solution color is observed after shaking the content for the same time. It means that there is a great synergistic effect between Fe_3O_4@Pd/$CaCO_3$-DTT NPs and US waves that make it essential to apply ultrasonic for reducing the antibodies. Images (b-d) suitably show Fe_3O_4@Pd/$CaCO_3$-DTT NPs (0.01 g), trastuzumab (8.0 µg/mL), and buffer phosphate (PBS, pH = 6.8) before ultrasonication, after ultrasonication for 10 min, and after magnetically collection of the magnetic NPs from the reaction mixture, respectively. Moreover, to show the best catalytic performance of the US' product, a comparison has been made between three different products obtained from reflux, MW and US irradiations methods (Fig. 10e). As can be seen, the US's product has exhibited the highest color transition to yellow, at the same conditions (ultrasonication, 50 KHz, 200 W, 10 min).

2.3.3. SDS-polyacrylamide gel electrophoresis

To monitor the reduction process of trastuzumab by the prepared Fe_3O_4@Pd/$CaCO_3$-DTT NPs, sodium dodecyl sulfate polyacrylamide gel electrophoresis (SDS-PAGE) test was performed. SDS-PAGE is an analytical method in biochemistry for identification and separation of the discrete proteins based on the molecule's charge and molecular masses in an electric field [30]. Thus, after completion of the reduction reaction of trastuzumab and separation of the magnetic NPs, purity and apparent molecular weight of purified trastuzumab was assessed by this method. As can be observed in Fig. 11, protein bands corresponding to the heavy (ca. 50 kDa) and light chains (ca. 25 kDa) were identified under reducing conditions (a), whereas ca. 190 kDa and a bit of fragmentation were observed under non-reducing conditions. Typically, a

Table 2
Optimization of the reaction conditions for disulfide bond reducing by Fe_3O_4@Pd/$CaCO_3$-DTT NPs, which were obtained via three different methods (reflux, MW, and US wave irradiation).

Entry	Product	Conditions	Cat. (g)	Time (min)	Yield[a] (%)
1	US	Ultrasonication (F: 50 KHz, PD: 200 W)	0.005	10	63
2	US	Ultrasonication (F: 50 KHz, PD: 200 W)	0.01	10	94*
3	US	Ultrasonication (F: 50 KHz, PD: 200 W)	0.05	10	95
4	US	Ultrasonication (F: 50 KHz, PD: 200 W)	0.01	20	93
5	US	Ultrasonication (F: 50 KHz, PD: 100 W)	0.01	30	88
6	US	Ultrasonication (F: 40 KHz, PD: 100 W)	0.01	10	77
7	US	Stirring at r.t.	0.01	10	75
8	MW	Ultrasonication (F: 50 KHz, PD: 200 W)	0.01	10	Trace
9	Reflux	Ultrasonication (F: 50 KHz, PD: 200 W)	0.01	10	69

* Optimum conditions.

[a] Isolated yields (purification was done via column chromatography); Diphenyl disulfide (2.0 mmol) in dry THF (4.0 mL), at room temperature (r.t.).

proper cassette for complex dialysis process is needed for separation of reducing agent and purification of the antibodies. While, this stage is practically jumped through using the heterogeneous Fe_3O_4@Pd/$CaCO_3$-DTT NPs with high paramagnetic property. Furthermore, different reducing conditions have been tested to investigate the synergistic catalytic effect between US waves and the fabricated Fe_3O_4@Pd/$CaCO_3$-DTT NPs, and also the best performance of the US's product rather than reflux's and MW's products. As shown in Fig. 11(b), the prepared Fe_3O_4@Pd/$CaCO_3$-DTT NPs seemed to be disable to completely reduce the TRA antibody. This observation proves that there is a great synergistic catalytic effect between US waves and the catalytic system. Additionally, Fig. 11 (c and d) have revealed that the products obtained via reflux and MW irradiation methods are not capable to reduce the antibodies in comparison with the US' product.

2.3.4. Recyclability

In order to investigate reusability of the Fe_3O_4@Pd/$CaCO_3$-DTT NPs, they were magnetically separated, washed with dry THF, and dried in a vacuum oven for 24 h, and used again in the model reaction (diphenyl disulfide reduction). As expected, after execution of a reduction reaction by the NPs, washing, and drying (recycling process), a significant decrease in the reaction yield was observed (Fig. 12, run 2). In fact, the active thiol sites of the loaded DTTs onto the NPs surfaces are oxidized during the reduction and recycling processes and need to be reactivated for the next running. For this purpose, a relatively concentrated DTT (0.1 M, in deionized water) was prepared and immediately used for activation of the NPs. Fe_3O_4@Pd/$CaCO_3$-DTT NPs were well dispersed and ultrasonicated in DTT solution for 10 min under neutral atmosphere, then separated and washed with dry THF, and freshly used for the next running. As shown in Fig. 12, the performance of the prepared Fe_3O_4@Pd/$CaCO_3$-DTT NPs in S-S bond reduction is acceptable after five times recycling, for US's product. A similar behavior was observed for recovered MW's product as well. It has been also shown that the efficiency of the US's product in S-S bond reduction reaction was totally higher than MW's product.

3. Experimental

3.1. Materials and equipment

All solvents, chemicals, and reagents were purchased from Sigma-Aldrich, as listed in Table S3 in the SI section. FT-IR spectra were obtained through (Shimadzu) FT-IR-8400 s, EDX spectra were recorded on VEGA-TESCAN-XMU, FESEM images were prepared with ZEISS SIGMA,

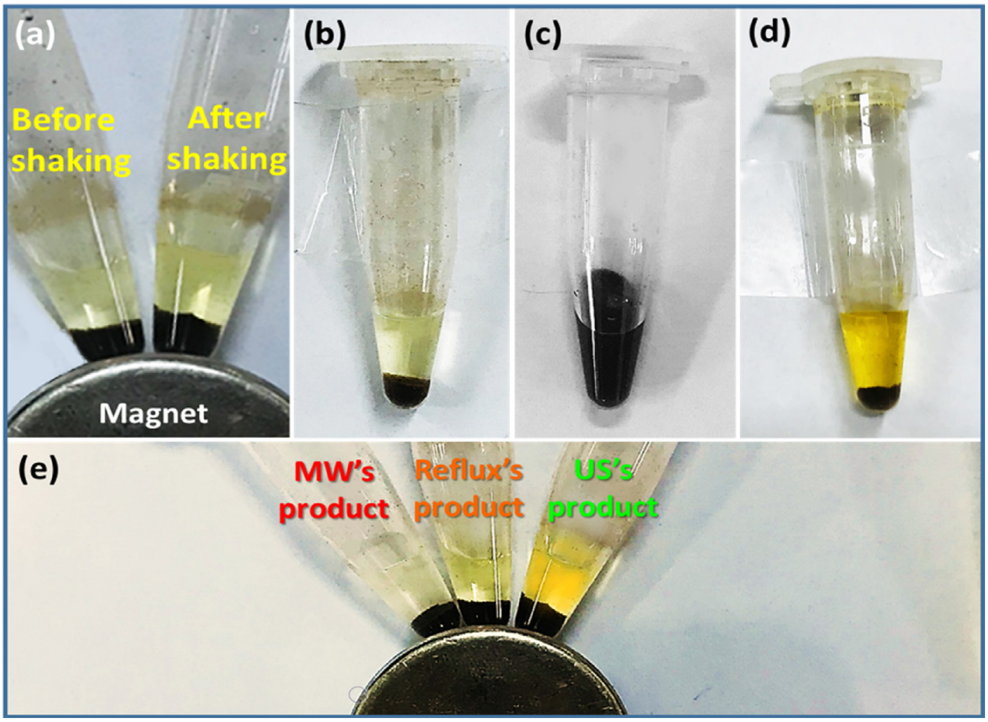

Fig. 10. The obtained colorimetric results from partial reduction of trastuzumab antibody by Fe_3O_4@Pd/$CaCO_3$-DTT NPs (US's product), in PBS (0.1 M, 6.8): (a) without the US radiation, (b) before ultrasonication, (c) after 10 min ultrasonication (50 KHz, 200 W), (d) after collection of the NPs by an external magnet, and (e) comparison of the catalytic performance between three different products from (MW, reflux and US irradiation methods) under US waves irradiation (10 min), in S-S bond reduction reaction.

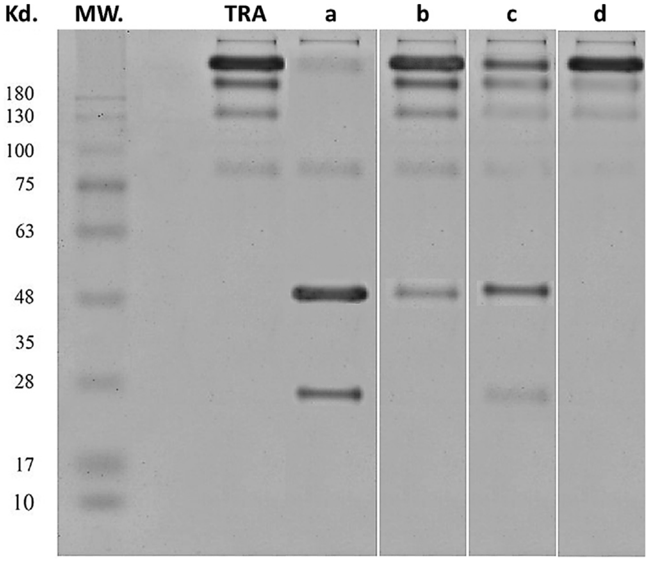

Fig. 11. SDS-PAGE analysis of trastuzumab (TRA, anti-HER2, IgG1) antibody under non-reducing conditions (TRA), and reducing conditions (a-d) provide by Fe_3O_4@Pd/$CaCO_3$-DTT NPs: (a) US's product (under ultrasonication), (b) US's product (shaking), (c) reflux's product (under ultrasonication), and (d) MW's product (under ultrasonication) [ultrasonication was carried out in an ultrasound bath with 50 KHz frequency and 200 W L^{-1} power density, for 10 min].

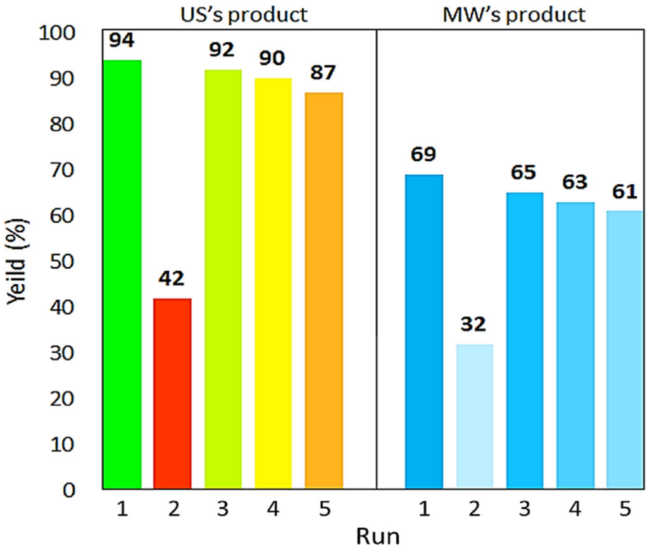

Fig. 12. Studying recyclability of the Fe_3O_4@Pd/$CaCO_3$-DTT NPs (obtained from US wave and MW irradiation methods), in the S–S bond reduction reaction of diphenyl disulfide.

a Horiba (SZ-100) equipped with a 658 nm laser and an avalanche photodiode detector (Perkin) was used to measure hydrodynamic diameters using dynamic light scattering (DLS). The XRD measurements were carried out by using a DRON-8 X-ray diffractometer, thermal analysis (TGA) was done by using of Bahr-STA 504 instrument under argon atmosphere, and the magnetic properties of sample were detected at room temperature using a VSM (Meghnatis Kavir Kashan Co., Kashan, Iran). A Shimadzu-UV-2550/220v solid-state UV–vis spectrometer was used to measure Uv–vis spectra, and the NMR spectra was prepared with Varian Unity Inova 500 MHz, and a Bruker Avance 300 MHz. An Eager 300 for EA1112 instrument was used for CHNS analysis. The statistical data of particle sizes from FESEM imaging and XRD analysis were obtained by Digimizer and Highscore plus software, respectively. Flash column chromatography was performed with silica gel (200–300 mesh). Analytical thin layer chromatography (TLC) was performed using Merck silica gel GF254 plates. Ultrasonic irradiation was performed in an ultrasound cleaning bath KQ-250 DE with a frequency of 50 kHz and power of 250 W L^{-1}. Prestained Protein Ladder (Fermentase-Russia), Coomasi blue staining solution, Bio-Rad-USA electrophoresis tank, and Whatman-USA paper filters were used for SDS-PAGE analysis. A conventional microwave oven (Godrej Microwave Oven, Model No- GMS 17M07WHGX) at a power of 1200 W was used.

3.2. Methods

3.2.1. Preparation of Fe_3O_4@SiO_2@Pd/$CaCO_3$ NPs

In a glass tube (Threaded Test Tube with Phenolic Cap, 13 × 100 mm), as-prepared Fe_3O_4@SiO_2 NPs (0.5 g) were well dispersed in dry tetrahydrofuran (THF, 7.0 mL) via ultrasonication for 10 min, at room temperature. Fe_3O_4@SiO_2 NPs were synthesized according to the procedure reported in our previous work [18–20]. In a separate flask, Pd/$CaCO_3$ (0.1 g, 1 mmol) was dissolved in THF (3.0 mL) and toluene (3.0 mL) via magnetically stirring for 1 h, at 80 °C, and after cooling down to room temperature was added to the glass tube. Next, the content of the glass tube was ultrasonicated (50 KHz) under N_2 atmosphere for 2 h, at room temperature. After completion of the reaction, the fabricated magnetic Fe_3O_4@SiO_2@Pd/$CaCO_3$ NPs were collected using an external magnet, washed with ethanol and acetone for several times, and dried at 60 °C.

3.2.2. US-assisted preparation of Fe_3O_4@Pd/$CaCO_3$-DTT NPs

In a glass tube, Fe_3O_4@SiO_2@Pd/$CaCO_3$ NPs (0.2 g) were well dispersed in dry ethanol via ultrasonication (10 min), then a solution of DTT (0.1 M in dry ethanol) was added drop by drop to the mixture over 20 min during the ultrasonication in an ice ultrasonic bath. After completion of the addition, the glass tube was well saturated of N_2 gas and sealed up with parafilm. Next, the mixture were ultrasonicated (50 KHz) at the same conditions for additional 10 min, then well washed with dry THF, and were immediately used in disulfide bond reduction reaction.

3.2.3. MW-assisted preparation of Fe_3O_4@Pd/$CaCO_3$-DTT NPs

1.0 g of Fe_3O_4@SiO_2@Pd/$CaCO_3$ NPs was weighed into a glass tube and well dispersed dry ethanol (8.0 mL) via ultrasonication (2 min). Then, a solution of DTT (0.1 M in dry ethanol) was added into the glass tube. The glass tube was well saturated of N_2 gas and sealed up with parafilm. Next, the mixture were subjected to microwave irradiation in a conventional microwave oven (300 W), for 1 h. Further, the NPs were magnetically collected and washed with dry THF.

3.2.4. S-S bond reduction by Fe_3O_4@Pd/$CaCO_3$-DTT NPs

In a glass tube (threaded test tube with phenolic cap, 13 by 100 mm), Fe_3O_4@Pd/$CaCO_3$-DTT NPs (0.01 g) were well dispersed in dry THF (4.0 mL) via ultrasonication for 50 min. Then, disulfide compound (2.0 mmol) was added and the glass tube was well charged of N_2 gas, and immediately sealed using phenolic cap and parafilm (the tube was evacuated and backfilled with nitrogen (this procedure was repeated three times). Next, the tube was put into an ultrasonic bath (under irradiation of US waves with 50 KHz frequency and power density = 200 W/L, at room temperature. After 10 min, the content of the glass tube was transferred to a beaker and the NPs were magnetically collected and washed with dry THF and reactivated by a DTT solution (0.1 M). The residue was concentrated through evaporation of THF and prepared for flash column chromatography.

3.2.5. SDS-polyacrylamide gel electrophoresis

8.0 µg of TRA antibody was subjected to a gradient 5–12% polyacrylamide gel under non-reducing and 5–20% gel after reduction. For reduction, 10% Fe_3O_4@Pd/$CaCO_3$-DTT NPs was added to the denaturating sample buffer and all samples were ultrasonicated for 10 min (F: 50 KHz and PD: 200 W), at room temperature. Then, the magnetic NPs were collected by an external magnet. Prestained Protein Ladder (Fermentase-Russia) were used to assess the approximate size of proteins.

3.2.6. Spectral data of produced thiol derivatives

Benzenethiol, as a colorless liquid (94% yield). ^{1}H NMR (500 MHz, DMSO): δ 7.55 (d, 2H), 7.41–7.44 (t, J = 5.0 Hz, 1H), 7.33–7.36 (t, 2H), 3.52 (bs, 1H) ppm. ^{13}C NMR (75 MHz, $CDCl_3$): δ 130.9, 129.5, 129.2, 115.7 ppm.

4-Chlorobenzenethiol, as a white solid (95% yield). ^{1}H NMR (300 MHz, $CDCl_3$): δ 7.20 (s, 4H), 3.45 (s, 1H) ppm. ^{13}C NMR (75 MHz, $CDCl_3$): δ 131.7, 130.8, 129.3, 129.2 ppm.

4-Methylbenzenethiol, as a colorless liquid (94% yield). ^{1}H NMR (300 MHz, $CDCl_3$): δ 7.20 (d, J = 8.1 Hz, 2H), 7.06 (d, J = 8.1 Hz, 2H), 3.40 (s, 1H), 2.31 (s, 3H) ppm. ^{13}C NMR (75 MHz, $CDCl_3$): δ 135.6, 129.9, 129.9, 126.6, 20.9 ppm.

4. Conclusions

One of the most important issues in antibody-drug conjugation is site-specification that directly influences on the drug release processes. In one way, drugs could be tagged on the antibodies through binding to the thiol sites provided from the reduced disulfide bonds. Since, almost complex purification processes like dialysis are needed to separate the reductant agent from the reduced antibody, a novel heterogeneous nanoscale reductant was designed and presented for this purpose in this study. Firstly, since they are prepared in nano scales, an extreme active surface area is provided by them and only partial amounts of them would be constructive for this purpose. Secondly, they could be conveniently separated from the mixture through their substantial paramagnetic property. Thus, dialysis process in which various types of membranes are used is practically eliminated from the antibody's reduction process. Herein, a convenient preparation strategy has been presented for the nanoscale S-S bond reductant, which is constructed of iron oxide NPs, silica network, Lindlar agent, and DTT (Fe_3O_4@Pd/$CaCO_3$-DTT). In this regard, ultrasonication has been introduced as the most efficient method, based on the obtained comparative data. Then, to evaluate the performance of the Fe_3O_4@Pd/$CaCO_3$-DTT NPs in the S-S bond reduction, a model reaction was considered for optimization of the reaction conditions. At this stage, column chromatography, TLC, and NMR were employed for purification, screening the reaction progress, and identification of the resulted product from reduction of diphenyl disulfide, respectively. High reaction yield (94%) in a short reaction time (10 min) was obtained via ultrasonication (50 KHz). Afterward, trastuzumab (anti-HER2), which is a humanized IgG1 antibody, was used to test the performance of the prepared Fe_3O_4@Pd/$CaCO_3$-DTT NPs in a real reduction reaction. Overall, both colorimetric experiment (by Ellman's reagent) and SDS-PAGE test have revealed that the great synergistic effect of Fe_3O_4@Pd/$CaCO_3$-DTT NPs and US waves could be a suitable alternative for homogeneous reducing agents and dialysis process for reduction of the antibodies.

Declaration of Competing Interest

The authors declare that they have no known competing financial interests or personal relationships that could have appeared to influence the work reported in this paper

Acknowledgements

The authors gratefully acknowledge the partial support from the Research Council of the Iran University of Science and Technology and the Iran National Science Foundation (INSF).

Appendix A. Supplementary data

The SI section includes EDX table, CHNS analysis table, applied materials table, TLC plates, and NMR spectra of produced thiol derivatives. Supplementary data to this article can be found online at https://doi.org/10.1016/j.ultsonch.2019.104824.

References

[1] K. Ninomiya, A. Fukuda, C. Ogino, N. Shimizu, Targeted sonocatalytic cancer cell injury using avidin-conjugated titanium dioxide nanoparticles, Ultrason. Sonochem. 21 (2014) 1624–1628.

[2] J.D. Bargh, A. Isidro-Llobet, J.S. Parker, D.R. Spring, Cleavable linkers in antibody–drug conjugates, Chem. Soc. Rev. 48 (2019) 4361–4374.

[3] K.E. Archer, E.E. Reid, M. Shizuka, J. Woods, L. Harris, E.K. Maloney, L.M. Bartle, O. Ab, A. Wilhelm, Y. Setiady, J.F. Ponte, R. Singh, T.A. Keating, R.V.J. Chari, M.L. Miller, Synthesis of highly potent N-10 amino-linked DNA-alkylating indolinobenzodiazepine antibody–drug conjugates (ADCs), ACS Med. Chem. Lett. 108 (2019) 1211–1215.

[4] N. Dan, S. Setua, V.K. Kashyap, S. Khan, M. Jaggi, M.M. Yallapu, S.C. Chauhan, Antibody-drug conjugates for cancer therapy: Chemistry to clinical implications, Pharmaceuticals 11 (2018) 32–42.

[5] A. Kumar, K. Kinneer, L. Masterson, E. Ezeadi, P. Howard, H. Wu, C. Gao, N. Dimasi, Characterization and *in vitro* data of antibody drug conjugates (ADCs) derived from heterotrifunctional linker designed for the site-specific preparation of dual ADCs, Data Brief. 21 (2018) 2208–2220.

[6] M.W. Handlogten, M. Zhu, S. Ahuja, Glutathione and thioredoxin systems contribute to recombinant monoclonal antibody interchain disulfide bond reduction during bioprocessing, Biotechnol. Bioeng. 114 (2017) 1469–1477.

[7] W.K. Chung, B. Russell, Y. Yang, M. Handlogten, S. Hudak, M. Cao, J. Wang, D. Robbins, S. Ahuja, M. Zhu, Effects of antibody disulfide bond reduction on purification process performance and final drug substance stability, Biotechnol. Bioeng. 114 (2017) 1264–1274.

[8] S. Paul, J. Connor, T. Nesspor, P. Haytko, K. Boakye, M.L. Chiu, H. Jiang, An efficient process of generating bispecific antibodies via controlled Fab-arm exchange using culture supernatants, Protein Expres. Purif. 121 (2016) 133–140.

[9] D.P. Facchi, A.L. Cazetta, E.A. Canesin, V.C. Almeida, E.G. Bonafé, M.J. Kipper, A.F. Martins, New magnetic chitosan/alginate/Fe_3O_4@SiO_2 hydrogel composites applied for removal of Pb(II) ions from aqueous systems, Chem. Eng. J. 337 (2018) 595–608.

[10] A. Maleki, R. Ghalavand, R. Firouzi Haji, Synthesis and characterization of the novel diamine-functionalized Fe_3O_4@SiO_2 nanocatalyst and its application for one-pot three-component synthesis of chromenes, Appl. Organomet. Chem. 32 (2018) e3916.

[11] S. Mallakpour, Z. Khani, Surface modified SiO_2 nanoparticles by thiamine and ultrasonication synthesis of PCL/SiO_2-VB1 NCs: Morphology, thermal, mechanical and bioactivity investigations, Ultrason. Sonochem. 41 (2018) 527–537.

[12] B.K. Sodipo, A. Abdul Aziz, One minute synthesis of amino-silane functionalized superparamagnetic iron oxide nanoparticles by sonochemical method, Ultrason. Sonochem. 40 (2018) 837–840.

[13] A.P. Cádiz Bedini, B. Klingebiel, M. Luysberg, R. Carius, Sonochemical synthesis of hydrogenated amorphous silicon nanoparticles from liquid trisilane at ambient temperature and pressure, Ultrason. Sonochem. 39 (2017) 883–888.

[14] R. Taheri-Ledari, J. Rahimi, A. Maleki, Synergistic catalytic effect between ultrasound waves and pyrimidine-2,4-diamine-functionalized magnetic nanoparticles: Applied for synthesis of 1,4-dihydropyridine pharmaceutical derivatives, Ultrason. Sonochem. 59 (2019) 104737.

[15] S.S. Maktedar, G. Avashthi, M. Singh, Ultrasound assisted simultaneous reduction and direct functionalization of graphene oxide with thermal and cytotoxicity profile, Ultrason. Sonochem. 34 (2017) 856–864.

[16] H. Liu, X.B. Hu, J.Y. Wang, R.I. Boughton, Structure, conductivity, and thermopower of crystalline polyaniline synthesized by the ultrasonic irradiation polymerization method, Macromolecules 35 (2002) 9414–9419.

[17] P. Zhang, M. Behl, X. Peng, M.Y. Razzaq, A. Lendlein, Ultrasonic cavitation induced shape-memory effect in porous polymer networks, Macromol. Rapid. Comm. 37 (37) (2016) 1897–1903.

[18] A. Maleki, R. Taheri-Ledari, M. Soroushnejad, Surface functionalization of magnetic nanoparticles via palladium-catalyzed Diels-Alder approach, Chemistryselect 3 (2018) 13057–13062.

[19] A. Maleki, R. Taheri-Ledari, J. Rahimi, M. Soroushnejad, Z. Hajizadeh, Facile peptide bond formation: Effective interplay between isothiazolone rings and silanol groups at silver/iron oxide nanocomposite surfaces, ACS Omega 4 (2019) 10629–10639.

[20] A. Maleki, M. Niksefat, J. Rahimi, R. Taheri-Ledari, Multicomponent synthesis of pyrano[2,3-d]pyrimidine derivatives via a direct one-pot strategy executed by novel designed copperated Fe_3O_4@polyvinyl alcohol magnetic nanoparticles, Mater. Today. Chem. 13 (2019) 110–120.

[21] A. Maleki, R. Taheri-Ledari, R. Ghalavand, R. Firouzi-Haji, Palladium-decorated o-phenylenediamine-functionalized Fe_3O_4/SiO_2 magnetic nanoparticles: A promising solid-state catalytic system used for Suzuki-Miyaura coupling reactions, J. Phys. Chem. Solids 136 (2020) 109200.

[22] N. Thavornsin, P. Chamrasboon, P. Kiatmongkolkul, R. Sakthanasait, M. Sukwattanasinitt, S. Wacharasindhu, Synthesis of highly pure poly

(aryleneethnylene)s using palladium supported on calcium carbonate as an eco-friendly heterogeneous catalyst, J. Polym. Sci. A 57 (2019) 1556–1563.

[23] W. Wang, Z. Wang, J. Wang, C.J. Zhong, C.J. Liu, Highly active and stable Pt–Pd alloy Catalysts synthesized by room-temperature electron reduction for oxygen reduction reaction, Adv. Sci. 4 (2017) 1600486.

[24] J. Li, H. Zhou, H. Zhuo, Z. Wei, G. Zhuang, X. Zhong, S. Deng, X. Li, J. Wang, Oxygen vacancies on TiO_2 promoted the activity and stability of supported Pd nanoparticles for the oxygen reduction reaction, J. Mater. Chem. A 6 (2018) 2264–2272.

[25] H.A. Al-Hosney, V.H. Grassian, Water, sulfur dioxide and nitric acid adsorption on calcium carbonate: A transmission and ATR-FTIR study, Phys. Chem. Chem. Phys. 7 (2005) 1266–1276.

[26] X.F. Qian, B. Li, Y.Y. Hu, G.X. Niu, D.Y. Zhang, R.C. Che, Y. Tang, D.S. Su, A.M. Asiri, D.Y. Zhao, Exploring meso-/microporous composite molecular sieves with core-shell structures, Chem 18 (2012) 931–939.

[27] Y. Zhang, M. Zhang, J. Yang, L. Ding, J. Zheng, J. Xu, S. Xiong, Formation of Fe_3O_4@SiO_2@C/Ni hybrids with enhanced catalytic activity and histidine-rich protein separation, Nanoscale 8 (2016) 15978–15988.

[28] W.W. Cleland, Dithiothreitol, a new protective reagent for SH groups, Biochemistry 3 (1964) 480–482.

[29] A. Béduneau, P. Saulnier, F. Hindré, A. Clavreul, J.C. Leroux, J.P. Benoit, Design of targeted lipid nanocapsules by conjugation of whole antibodies and antibody Fab' fragments, Biomaterials 28 (2007) 4978–4990.

[30] H. Liu, G. Gaza-Bulseco, C. Chumsae, A. Newby-Kew, Characterization of lower molecular weight artifact bands of recombinant monoclonal IgG1 antibodies on non-reducing SDS-PAGE, Biotechnol. Lett. 11 (2007) 1611–1622.